

Assessment of the Aggregation State of Integral Membrane Proteins in Reconstituted Phospholipid Vesicles Using Small Angle Neutron Scattering

John F. Hunt¹, Pierre D. McCrea¹, Giuseppe Zaccai^{2,3}
and Donald M. Engelman^{1*}

¹Department of Molecular Biophysics and Biochemistry
Yale University, New Haven
CT 06511, USA

²Institut de Biologie Structurale J.-P. Ebel
CEA/CNRS, 41 Avenue des
Martyrs 38027 Grenoble
CEDEX 1, France

³Institut Laue Langevin
Avenue des Martyrs, BP 156
38042 Grenoble CEDEX 9
France

The assessment of the physical size of integral membrane protein complexes has generally been limited to samples solubilized in non-ionic detergent, a process which may introduce artifacts of unknown scope and severity. A system has been developed that allows observation of the small angle scattering profile of an integral membrane protein while incorporated in small unilamellar phospholipid vesicles. Contrast matching of isotopically substituted phospholipid eliminates the contribution of the bilayer to the observed scattering, resulting in a profile dependent only on the structure of the individual membrane protein complexes and their spatial arrangement in the vesicle. After appropriate compensation for their spatial arrangement, information about the molecular mass and radius of gyration of the individual complexes can be obtained. The validity of the approach has been established using monomeric bacteriorhodopsin as a model system.

© 1997 Academic Press Limited

*Corresponding author

Keywords: small angle neutron scattering; membrane proteins; phospholipid vesicles; aggregation state; bacteriorhodopsin

Introduction

Many important biological processes involve the association of protein molecules or subsegments of protein molecules in the phospholipid bilayer of cellular membranes. For example, the folding of integral membrane proteins depends on structural interactions in this environment (Popot & Engelman, 1990; le Maire, 1986). Moreover, associations between integral membrane proteins play an important functional role in many physiological processes (Hurtley & Helenius, 1989; Bormann &

Engelman, 1992; Manolios *et al.*, 1990). For many cell surface receptors, the transduction of extracellular signals to the cytoplasm is believed to be mediated by reversible oligomerization reactions (Heldin, 1995; Ullrich & Schlessinger, 1990; Wells, 1994). Although this model is supported by a large body of inferential experimental data, physical evidence of oligomer formation in the membrane is still weak because of the problems inherent in studying associations within cellular membranes (Gennis, 1989; Carraway *et al.*, 1989; Carraway & Cerione, 1991). To date, the most direct evidence for such interactions comes from crystal structure analysis of complexes between ligands and soluble fragments of receptors which have had their membrane-spanning domains excised (de Vos *et al.*, 1992; Livnah *et al.*, 1996).

Experimental studies of the association of protein domains in the phospholipid bilayer have generally employed either chemical cross-linking *in situ* (Gaffney, 1985; Cochet *et al.*, 1988; Heegaard *et al.*, 1990) or hydrodynamic analysis of detergent-solubilized membranes (Tanford & Reynolds, 1976; le Maire *et al.*, 1986; Casey & Reithmeier, 1991; Møller *et al.*, 1988). Chemical cross-linking has produced misleading results in at least one system, which was later characterized using scattering

Present addresses: J. F. Hunt, Department of Biological Sciences, Columbia University, New York, NY 10027, USA; P. D. McCrea, Department of Biochemistry and Molecular Biology, University of Texas M. D. Anderson Cancer Center, Houston, TX 77030-4095, USA.

Abbreviations used: bR, bacteriorhodopsin; β -og, β -octylglucoside; CHB, chloride HPLC buffer; DMPC, dimyristoylphosphatidylcholine; HPLC, high-performance liquid chromatography; $I(0)$, intensity scattered at zero angle; IMP, integral membrane protein; Mega-8, octanoyl-*N*-methylglucamide; Q , $4\pi\sin\theta/\lambda$; R_g , radius of gyration; SANS, small angle neutron scattering; TX-100, Triton X-100.

techniques (Capel *et al.*, 1987), while detergent solubilization of membranes may introduce structural perturbations of unknown scope and severity (Tanford & Reynolds, 1976; le Maire, 1986). Alternatives to these approaches have been fluorescence resonance energy transfer (Veatch & Stryer, 1977; Carraway *et al.*, 1989; Carraway & Cerione, 1991) and target size analysis by radiation inactivation (le Maire *et al.*, 1990); both of these techniques are sensitive to an array of experimental artifacts.

Because of the difficulties and ambiguities inherent in all of the existing experimental approaches, we have explored the feasibility of using small angle neutron scattering (SANS) (Jacrot, 1976) to characterize the physical size of integral membrane protein complexes reconstituted into phospholipid vesicles. A small unilamellar phospholipid vesicle will typically have a molecular mass between 2×10^6 and 3×10^7 daltons and contain only 1% to 20% protein by weight (Racker *et al.*, 1979; Gennis, 1989). Because of the overwhelming preponderance of phospholipid compared with protein as well as the large size of the vesicles compared with individual protein molecules, it would be effectively impossible to observe scattering from the protein if all of the components in the vesicle had equal contrast. Nonetheless, it should be possible to use neutron scattering in conjunction with solvent contrast variation (Ibel & Stuhrmann, 1975; for a review, see Zaccai & Jacrot, 1983) to selectively suppress small angle scattering from the phospholipid and thereby allow direct observation of the protein in the reconstituted vesicles.

A variety of theoretical and practical experimental complications must be considered when applying neutron scattering techniques to objects of such chemical and geometrical complexity. Therefore, before attempting to characterize a system involving integral membrane protein folding or oligomerization, it was necessary to explore the technical obstacles using a simple model system in order to determine whether it is possible to obtain an accurate estimate of the molecular weight and the radius of gyration for an integral membrane protein *in situ* in phospholipid vesicles. For this purpose, we chose the well-characterized protein bacteriorhodopsin (bR) which is a light-driven transmembrane proton pump (Oesterhelt & Stoerkenius, 1971; Khorana, 1988) and has served as a structural prototype for the ubiquitously distributed seven-helix receptors from eukaryotic cells (Findlay *et al.*, 1993). This protein offers the additional advantage that its three-dimensional structure has been determined at approximately 3.5 Å resolution using electron crystallography (Grigorieff *et al.*, 1996).

The most straightforward way of using the contrast variation technique is to make scattering measurements with the contrast level (i.e. the scattering length density) of the solvent adjusted to match the contrast level of the species whose scat-

tering is to be suppressed, which effectively renders this species "invisible" in the scattering experiment. Therefore, in applying this technique to reconstituted vesicles, protein scattering profiles can be measured in buffers adjusted to the contrast match point of the relevant phospholipid. An important limitation is that the scattering density of the species to be matched (i.e. the phospholipid bilayer) should be as homogeneous as possible, because deviations from the mean contrast value will contribute to the observed signal. Deuterated phospholipids were used in the neutron scattering experiments rather than protonated phospholipids in order to make the scattering density distribution within the bilayers more homogeneous as well as to optimize the signal-to-noise in the measurements. The patterns of deuteration in these synthetic phospholipids are shown in Figure 1. The neutron contrast level of fully protonated dimyristoyl-phosphatidylcholine (DMPC) is equivalent to that in an aqueous buffer containing 11% $^2\text{H}_2\text{O}$ while the neutron contrast level of the deuterated phospholipids is equivalent to that in either 94% $^2\text{H}_2\text{O}$ (d_{63} -DMPC) or 99% $^2\text{H}_2\text{O}$ (d_{67} -DMPC). In principle, protein scattering profiles could be measured in either environment because the neutron contrast level of a typical protein molecule is equivalent to that in 42% $^2\text{H}_2\text{O}$ (Ibel & Stuhrmann, 1975). However, neutron scattering measurements in the presence of a high concentration of $^1\text{H}_2\text{O}$ are complicated by an intense background of incoherently scattered (i.e. phase-randomized) neutrons (Jacrot, 1976). Furthermore, a slightly higher protein contrast level is obtained in the two buffers containing high concentrations of $^2\text{H}_2\text{O}$.

In a physical system of this complexity, scattering experiments can be compromised by a variety of interference effects (Malfois *et al.*, 1996; Veretout *et al.*, 1989). In our experiments with vesicles containing bR, we have systematically addressed the three most important sources of error in order to ensure that we are observing an undistorted scattering profile for an individual protein molecule.

Theoretical Considerations

Protein-protein correlations in a phospholipid vesicle

Protein-protein correlations within a single vesicle will certainly contribute to the observed scattering profiles for low values of the scattering angle Q . Qualitatively, the intensity at very low Q should be dominated by the arrangement of protein monomers in the vesicle, while, under certain circumstances, the intensity in an intermediate Q -range should represent a relatively undistorted small angle scattering profile for the isolated protein monomer (Glatter & Kratky, 1982; Curmi *et al.*, 1988).

As the basis for a quantitative description of the experiment, consider the scattering profile of a

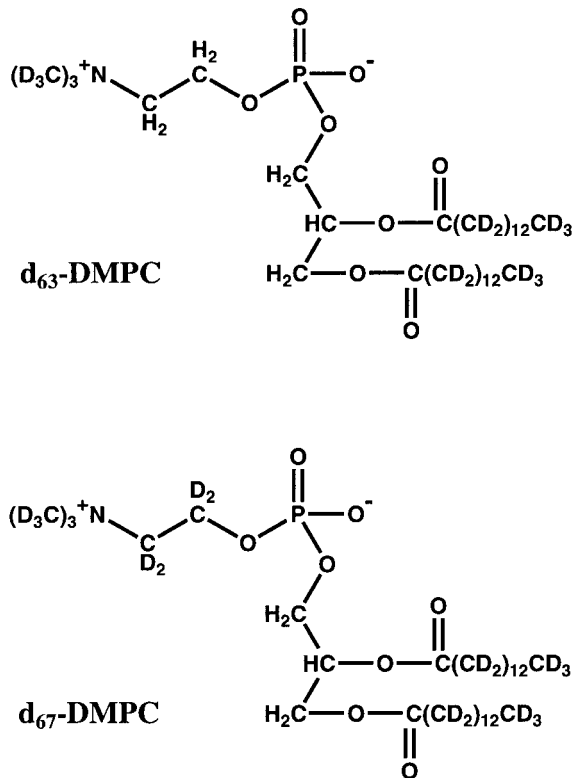


Figure 1. Patterns of deuteration in the synthetic DMPCs used in the SANS experiments.

single vesicle in a specific orientation with a specific distribution of protein monomers (Feigin & Svergun, 1987; Guinier, 1963):

$$I(Q) = \sum_{i,j} f_i f_j^* e^{i\mathbf{Q}\cdot\mathbf{R}_{ij}} = \sum_i |f_i|^2 + \sum_{i \neq j} f_i f_j^* e^{i\mathbf{Q}\cdot\mathbf{R}_{ij}}$$

In this equation, $I(Q)$ is the intensity of the scattered radiation as a function of scattering angle ($Q = 4\pi \sin\theta/\lambda$), f_i is the structure factor of the monomer, which is a complex number dependent on the orientation of the protein molecule, and \mathbf{R}_{ij} is a vector from the center of monomer i to the center of monomer j . (Combination of the terms i,j and j,i in the second sum on the right-hand side of the equation yields a real-valued function, consistent with its description of an intensity.) Note that the scattered intensity described by this equation is a linear function of the pairwise interference terms $f_i f_j^* e^{i\mathbf{Q}\cdot\mathbf{R}_{ij}}$. Although there will only be a limited number of pairwise interactions in any single vesicle, the linearity of the intensity function can be exploited to average the interference function over all of the vesicles in the sample.

The number of pairwise interactions in a vesicle containing n protein molecules is given by $1/2(n^2 - n)$, which is approximately equal to $1/2n^2$ for large n . Thus, we can average the intensity function over all of the vesicles V_k with a given size and shape in the following manner:

$$I(Q) \cong m_k \cdot d_s \cdot A_k \cdot \langle |f_i|^2 \rangle + \frac{m_k}{2} (d_s \cdot A_k)^2 \langle f_i f_j^* e^{i\mathbf{Q}\cdot\mathbf{R}_{ij}} \rangle_{V_k}$$

In this equation, d_s represents the surface density of protein in vesicles in the sample (a function of the lipid-to-protein ratio), A_k represents the surface area of each vesicle V_k , and m_k represents the number of vesicles V_k in the sample. Based on these relationships, $n_k = d_s \cdot A_k$. Given the fact that there are at least 10^{15} vesicles in the neutron beam during a measurement, it is possible to use an ensemble average of this kind. Assuming a random orientation of vesicles in the sample, the term $\langle |f_i|^2 \rangle$ represents the orientationally averaged small angle scattering profile of the protein monomer.

The experimentally observed intensity will equal the sum of the intensity contributed by vesicles of all different sizes and shapes:

$$I(Q) = d_s \cdot \left(\sum_k m_k \cdot A_k \right) \cdot \langle |f_i|^2 \rangle + d_s^2 \cdot \frac{1}{2} \times \left(\sum_k m_k \cdot A_k^2 \cdot \langle f_i f_j^* e^{i\mathbf{Q}\cdot\mathbf{R}_{ij}} \rangle_{V_k} \right)$$

The total number of protein molecules in the sample is described by the following expression:

$$N = \sum_k m_k \cdot d_s \cdot A_k = d_s \cdot \sum_k (m_k \cdot A_k)$$

Finally, the observed scattering intensity can be normalized to protein concentration:

$$I(Q)/N = \langle |f_i|^2 \rangle + d_s \cdot \frac{1}{2} \times \left(\sum_k \left(\frac{m_k \cdot A_k}{\sum_k m_k \cdot A_k} \right) \cdot A_k \cdot \langle f_i f_j^* e^{i\mathbf{Q}\cdot\mathbf{R}_{ij}} \rangle_{V_k} \right)$$

Thus, the observed intensity should be given by the sum of the scattering profile of the monomer plus an interference term which is linearly proportional in magnitude to the surface density of protein in the vesicles. Therefore, all inter-protein interference terms within an individual vesicle tend toward zero in the limit as the surface density of the protein is reduced. On this basis, we conclude that intra-vesicular interference effects are negligible compared with the small angle scattering from the isolated monomer in any Q -range in which the normalized scattering profile is independent of the lipid-to-protein ratio in the sample.

Lack of match in detail

Distortions can be introduced into the scattering profile due to interference between the protein molecule and the residual fluctuation of scattering length density in the phospholipid bilayer. Although the average scattering length density of the phospholipid is equal to the scattering length

density of the solvent, the contrast level inside the bilayer is not matched in detail. Specifically, the scattering length density in the hydrophobic core of the bilayer in the vesicles is slightly higher than that of the solvent, while the scattering length density in the headgroup region is slightly lower. These fluctuations in the scattering length density of the bilayer occur on a length scale of approximately half the thickness of the bilayer ($d \sim 15 \text{ \AA}$). Since interference effects should only become significant at values of $Q \geq \pi/d \sim 0.2$, we do not expect them to be significant in the Q -range in which we have analyzed our experimental data, i.e. $Q \leq 0.10$ (for reviews, see Feigin & Svergun, 1987; Glatter & Kratky, 1982). Moreover, the contrast within the bilayer is very weak compared with the contrast between the protein and the deuterated lipid.

Nonetheless, the volume of the bilayer greatly exceeds the volume of the protein molecules in a reconstituted vesicle, and the geometric arrangement of the scattering length density in the vesicle is fairly complex. In this context, we thought that it would be advisable to address the possibility of protein-lipid interference effects experimentally. Therefore, we have performed a complete set of neutron scattering experiments with bR reconstituted into phospholipid vesicles made from two different kinds of isotopically substituted dimyristoylphosphatidylcholine (DMPC), i.e. d_{63} -DMPC and d_{67} -DMPC (Figure 1). These vesicles should have substantially different scattering length density profiles across the bilayer (Zaccai *et al.*, 1979; Büldt *et al.*, 1978, 1979; Wiener & White, 1992), so that we would expect to observe a difference between the data acquired in the two phospholipids if protein-lipid interference effects make a significant contribution to the observed neutron scattering profile of the protein. Since the protein scattering profiles measured in these two environments look identical, we conclude that the contribution of these interference effects are negligible in this system in the relevant Q -range (see Figure 6, below).

Results

Contrast matching of deuterated phospholipids

Vesicles were made from one of two isotopic variants of DMPC containing different levels of deuteration in their choline headgroup: d_{63} -DMPC and d_{67} -DMPC (Figure 1). The results of experiments to determine the contrast match point of d_{63} -DMPC are shown in Figure 2(a), which shows scattering profiles measured from pure lipid vesicles in buffers containing varying amounts of $^2\text{H}_2\text{O}$; all profiles are scaled to a phospholipid concentration of 100 mg/ml. The contrast match point is given by the $^2\text{H}_2\text{O}$ concentration at which the intensity of neutrons scattered in the forward direction goes to zero, i.e. $I(0) = 0$. Because $I(0)$ values cannot be measured directly, they must be

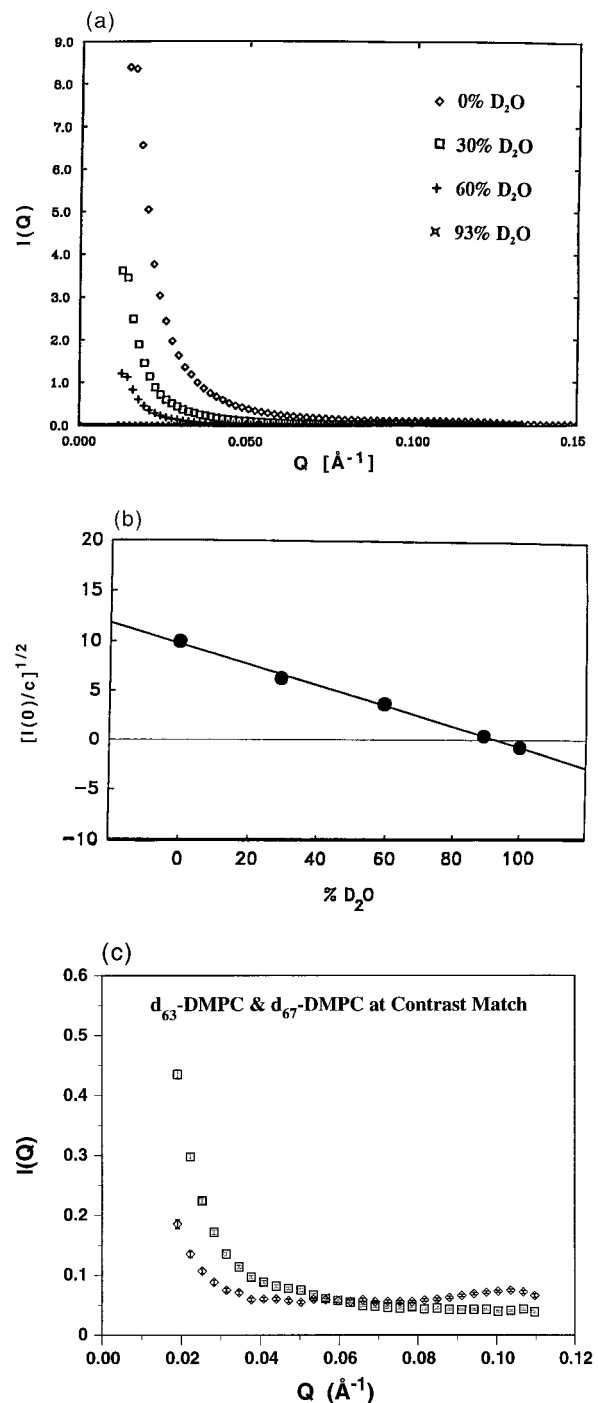


Figure 2. Contrast matching of pure phospholipid vesicles. (a) Small angle scattering profiles of d_{63} -DMPC vesicles measured in buffers containing different concentrations of $^2\text{H}_2\text{O}$ (D_2O). All of the profiles are scaled to a phospholipid concentration of 100 mg/ml. (b) Plot of the estimated forward scatter of the vesicles (i.e. $I(0)$) as a function of the solvent contrast level. The data are plotted in the format $[I(0)/c]^{1/2}$ versus $\% \text{D}_2\text{O}$, where c represents the concentration of phospholipid. The procedure used to determine the $I(0)$ values from the data in (a) is described in the text. (c) SANS profiles of pure phospholipid vesicles at their nominal contrast match points: 94% $^2\text{H}_2\text{O}$ for d_{63} -DMPC (\diamond) and 99% $^2\text{H}_2\text{O}$ for d_{67} -DMPC (\square); the profiles are scaled to a phospholipid concentration of 100 mg/ml. Error bars representing ± 1 standard deviation are shown.

determined by extrapolation of the observed scattering profiles to zero angle. According to the approximation of Guinier (1963), the scattering profile should be linear at small angles when plotted in the form $\ln[I(Q)]$ versus Q^2 , although this relationship is rigorously observed only for values of $Q \leq R_g^{-1}$ (Feigin & Svergun, 1987). The R_g , or radius of gyration, of the vesicles used in these experiments is at least 250 Å, meaning that the Guinier approximation strictly applies only to angles with $Q \leq 0.004$, i.e. only to angles smaller than those accessible in our experiments. Nonetheless, replotting the data in Figure 2(a) in the Guinier format yielded straight lines at low Q values for all of the scattering profiles (data not shown), indicating that it is possible to approximate this local segment of the scattering profile of the pure lipid vesicles as a Gaussian function. Least-squares regression was used to extrapolate these lines to zero angle, yielding pseudo- $I(0)$ values for the samples. The square-root of these pseudo- $I(0)$ values are plotted as a function of $^2\text{H}_2\text{O}$ concentration in Figure 2(b); the linear relationship observed in this graph indicates that the extrapolation procedure is robust enough to yield intensity values which have the correct functional dependence on the solvent contrast level.

The position of the intercept of the line in Figure 2(b) on the abscissa indicates that the contrast match point of d_{63} -DMPC vesicles is approximately 94% $^2\text{H}_2\text{O}$. An equivalent set of experiments performed with d_{67} -DMPC vesicles indicates that the contrast match point of this lipid species is approximately 99% $^2\text{H}_2\text{O}$ (data not shown). Because of potential inaccuracies in the procedure used to determine the contrast match points, additional experiments were performed to define the values more accurately, as well as to characterize the sensitivity of the scattering profiles to perturbations in the exact solvent contrast level. For each of the two deuterated lipid species, scattering profiles were measured from a sample in which the solvent $^2\text{H}_2\text{O}$ content was varied systematically in 0.5% steps within $\pm 2\%$ of the nominal contrast match point (by adding small aliquots of $^1\text{H}_2\text{O}$ or $^2\text{H}_2\text{O}$ buffer directly to the vesicle sample in the cuvette). No significant change was observed in the scattering profile of either lipid species for variations in $^2\text{H}_2\text{O}$ content within $\pm 1\%$ of the nominal contrast match point (data not shown).

Figure 2(c) compares the residual scatter of d_{63} -DMPC vesicles and d_{67} -DMPC vesicles at their respective contrast match points. Although the intensity of neutron scattering by the vesicles is dramatically suppressed, some residual scattering is observed in this Q -range. There are a number of possible explanations for the physical origin of this signal. The first possibility is that it could derive from a very small mismatch between the mean scattering length density of the buffer and the bilayer, which would produce an appreciable signal because of the massive size of the vesicles, although the insensitivity of the residual scattering

profile to small variations in $^2\text{H}_2\text{O}$ concentration tends to weigh against this explanation. The second possibility is that the residual signal could derive from some heterogeneity in the physical state of the phospholipid. DMPC multilayers would be expected to have a slightly different contrast match point from DMPC bilayers because these phases differ in their specific volume and water binding properties (Marsh, 1990; Bendzko *et al.*, 1988); therefore, a low concentration of multilayers in the vesicle solution (Knoll *et al.*, 1981) could give rise to coherent neutron scattering, even at zero angle. Dynamic fluctuations in bilayer density could also produce coherent scatter at zero angle, although the fluctuations would have to modulate the mean density of an entire vesicle. The final possibility is that some of the residual signal could derive from incoherent or phase-randomized scatter. Even though the coherent scattering length density of the buffer and the bilayer is matched, there may be a mismatch in their incoherent scattering length density because their chemical and therefore isotopic composition is different (Lehmann & Zaccai, 1984); this effect would contribute a background of neutron intensity which is independent of the scattering angle. We have not pursued a deeper analysis of the physical origin of the residual scatter from the phospholipid vesicles at their nominal contrast match point because the data presented below show that this signal can be effectively subtracted from the observed scattering profiles of protein-containing vesicles.

Scattering profiles from protein-containing vesicles at the lipid contrast match point

Figure 3 shows small-angle neutron scattering profiles of vesicles containing bR compared with pure phospholipid vesicles. All of the profiles were measured at the nominal contrast match point of the phospholipid and scaled to a phospholipid concentration of 100 mg/ml (after buffer subtraction). Data for d_{63} -DMPC vesicles and d_{67} -DMPC vesicles are shown in Figure 3(a) and (b), respectively. For each lipid species, data are shown for vesicles containing two different weight ratios of lipid relative to protein. Variation in the lipid-to-protein ratio is achieved by mixing protein-containing vesicles with pure lipid vesicles and performing two rounds of freeze/thaw followed by sonication. Data are shown for the vesicles containing the highest and the lowest protein concentrations used in the experiments (approximately a 6:1 and 15:1 weight ratio of lipid-to-protein). Although it is obvious that the protein-containing vesicles scatter neutrons very strongly compared with pure lipid vesicles, the magnitude of the residual scatter from the phospholipid is too large to be ignored, especially for the samples at the highest lipid-to-protein ratios. Therefore, this signal must be subtracted from the scattering profiles of

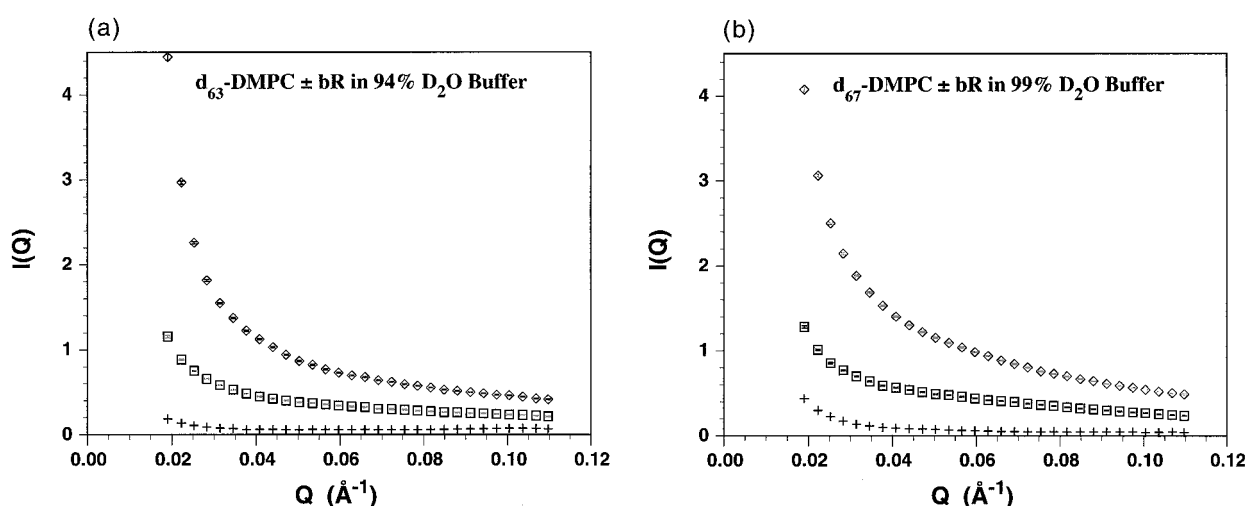


Figure 3. SANS profiles of bR vesicles at the contrast match point of the phospholipid. Profiles are shown for vesicles at two different lipid-to-protein weight ratios (6:1 (\diamond) and 15:1 (\square)) as well as for pure lipid vesicles (+). All of the profiles are normalized to a DMPC concentration of 100 mg/ml. The concentration of phospholipid in these samples was approximately 70 mg/ml. Error bars representing ± 1 standard deviation are shown. (a) Profiles of samples in d_{63} -DMPC measured in a buffer containing 94% $^2\text{H}_2\text{O}$. (b) Profiles of samples in d_{67} -DMPC measured in a buffer containing 99% $^2\text{H}_2\text{O}$.

the protein-containing vesicles before the structural parameters of the protein can be evaluated.

Intervesicular interference effects

Interparticle interference effects frequently distort the small angle scattering profiles observed for macromolecules and macromolecular complexes in aqueous solution (for reviews, see Zaccai & Jacrot, 1983; Feigin & Svergun, 1987; Glatter & Kratky, 1982). These effects arise from spatial correlations between the scattering particles, which leads to interference of the radiation scattered from different particles. As discussed

above, in scattering experiments with reconstituted vesicles, interparticle interference can arise either from correlations between the scattering species in different vesicles (inter-vesicular interference) or from correlations between the scattering species in a single vesicle (intra-vesicular interference).

Inter-vesicular interference effects can be examined by diluting vesicles with buffer in order to determine the effect of vesicle concentration on the observed scattering profile. Figure 4(a) shows buffer-subtracted SANS profiles of pure d_{63} -DMPC vesicles at four different concentrations 33 mg/ml and 8 mg/ml; these profiles are all

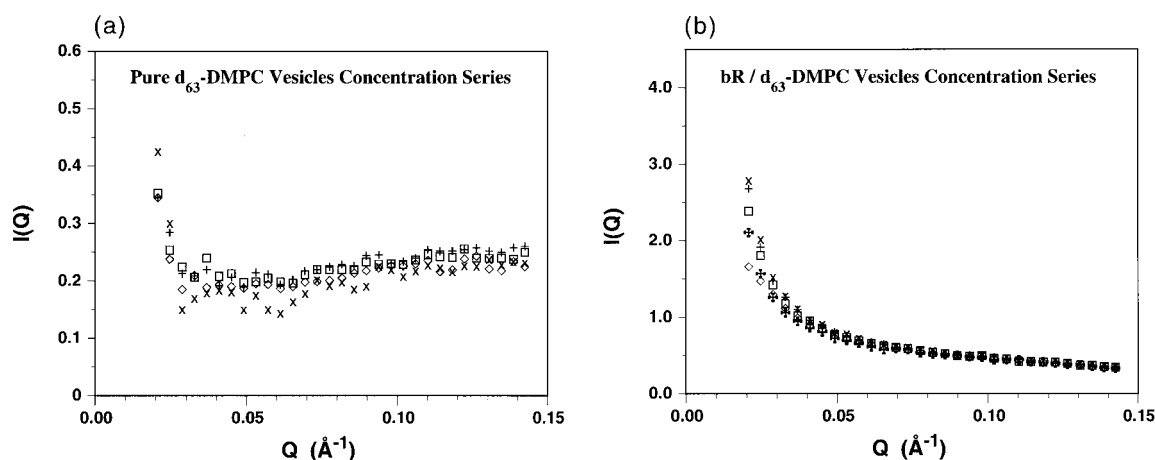


Figure 4. Vesicle concentration series measured in 93% $^2\text{H}_2\text{O}$. The sample containing the highest concentration of the vesicles was measured first, and it was progressively diluted with dialysis buffer to produce the samples at lower concentration. (a) Pure d_{63} -DMPC vesicles measured at 33 mg/ml (\diamond), 25 mg/ml (\square), 17 mg/ml (+), and 8 mg/ml (\times). All of the profiles are scaled to a phospholipid concentration of 200 mg/ml. (b) Lipid-subtracted profiles of vesicles containing bR at a 10:1 lipid-to-protein weight ratio in d_{63} -DMPC. All of the profiles are scaled to a protein concentration of 10 mg/ml. The phospholipid concentrations in the samples were: 44 mg/ml (\diamond , \boxtimes), 33 mg/ml (\square), 22 mg/ml (+), and 11 mg/ml (\times).

scaled to a lipid concentration of 200 mg/ml. The residual scatter of the phospholipid is concentration-independent over the entire Q -range (0.025 to 0.15). However, the observed scattering profile of bR in d_{63} -DMPC vesicles is dependent on the concentration of the vesicles, as shown by the data in Figure 4(b). This panel shows lipid-subtracted SANS profiles of bR vesicles containing a 10:1 weight ratio of lipid-to-protein measured at four different vesicle concentrations. The profiles were acquired at phospholipid concentrations between 44 mg/ml and 11 mg/ml and eventually all scaled to a protein concentration of 10 mg/ml. A suppression of the small angle scattering of the protein is observed at $Q \leq 0.04$ in the samples containing higher concentrations of the vesicles.

An effect of this kind is observed in many highly concentrated systems because of short-range order (Malfois *et al.*, 1996; Tardieu *et al.*, 1992; Veretout *et al.*, 1989). Under these conditions, any tendency of the constituents to avoid one another due to electrostatic repulsion or excluded volume effects will cause their spatial locations to be correlated. In this situation, the suppression of the scattering intensity at low Q can be rationalized in a qualitative sense based on the statistical tendency of the particles to form a "pseudo-lattice" due to mutual avoidance (Zaccai & Jacrot, 1983). The substantially stronger interference observed for the bR vesicles compared with the electrostatically neutral pure phospholipid vesicles suggests that the effect could be mediated by electrostatic repulsion; the bR vesicles are expected to carry a significant net surface charge because the asymmetrical orientation of the protein leads to preferential exposure of its anionic carboxy terminus on the external surface of the DMPC vesicles (Huang *et al.*, 1980). In any event, analysis of the structural parameters of the protein

in the reconstituted vesicles will have to be restricted to data points at $Q \geq 0.04$, where the protein scattering profile is independent of vesicle concentration.

Intravesicular interference effects

Intravesicular interference can be examined by varying the lipid-to-protein ratio in the vesicles because the surface density of the protein is essentially inversely proportional to the lipid-to-protein ratio. This variation was accomplished by mixing protein-containing vesicles with pure lipid vesicles and then fusing them by two rounds of freeze/thaw/sonication prior to remeasuring their scattering profile. Figure 5(a) and (b) shows lipid-subtracted SANS profiles of bR at four different lipid-to-protein ratios in d_{63} -DMPC or d_{67} -DMPC, respectively. In both lipid environments there is a strong interference phenomenon resulting in increased scattering intensity at low angle as the surface density of the protein increases in the vesicles. However, the scattering intensity is independent of the lipid-to-protein ratio at $Q \geq 0.05$ in the d_{63} -DMPC vesicles and at $Q > 0.06$ in the d_{67} -DMPC vesicles.

This behavior is exactly what is expected in this system based on the theoretical considerations outlined above. The constructive interference observed at low angles is attributable to the arrangement of the protein molecules in the phospholipid vesicles and reflects the overall size and shape of the vesicles. (We estimate that there are between 200 and 500 bR monomers per vesicle under the conditions of these experiments.) However, intravesicular protein-protein correlations cannot contribute to the scattering profiles in the Q -range where the observed intensity is independent of the surface

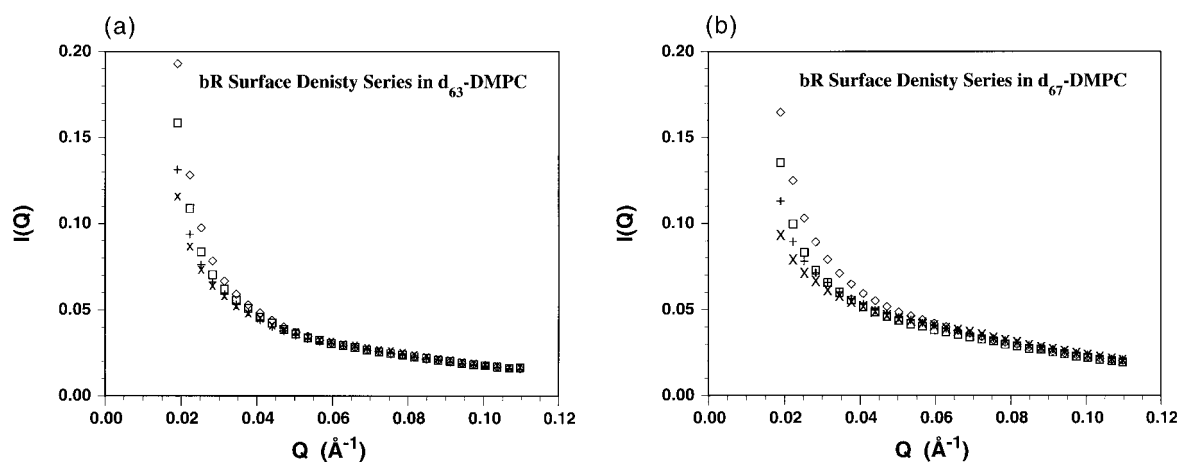


Figure 5. Protein surface density series. SANS profiles of bR vesicles at four different lipid-to-protein weight ratios: 6:1 (\diamond), 9:1 (\square), 12:1 (+), and 15:1 (\times). The vesicles at the lowest lipid-to-protein ratio (6:1) were measured first and then fused with pure lipid vesicles to produce the vesicles at higher lipid-to-protein ratios (see Materials and Methods). All of the profiles are scaled to a protein concentration of 0.8 mg/ml. The phospholipid concentration in these samples was approximately 70 mg/ml. (a) bR in d_{63} -DMPC vesicles measured in a buffer containing 94% $^2\text{H}_2\text{O}$. (b) bR in d_{67} -DMPC vesicles measured in a buffer containing 99% $^2\text{H}_2\text{O}$.

density of the protein in the vesicles. Therefore, the scattering profile in this region reflects the size and shape of the protein molecule (including its oligomeric structure).

Figure 6 presents a review of the protocol used to process the small angle scattering profiles of reconstituted vesicles measured at the nominal contrast match point of the phospholipid. Samples are measured at a series of lipid-to-protein ratios (and at least one of these samples is measured at a series of vesicle concentrations). The raw data are corrected for the background scattering of the buffer, the sample transmission, and the electronic background using standard techniques (Ibel, 1976; Ghosh, 1989). Next, all of the profiles are scaled to the same phospholipid concentration (Figure 3), and the scattering profile of the pure lipid vesicles is subtracted from the scattering profile of each sample of protein-containing vesicles. Finally, the lipid-subtracted profiles are scaled to the same protein concentration (Figures 6(b) and 7). These profiles represent the small angle neutron scattering of the protein component in the reconstituted vesicles and reflect the size and shape of the protein molecule as well as its arrangement in the vesicles. As described in the preceding paragraph, analysis of the profiles acquired from samples at different lipid-to-protein ratios allows determination of the relative contribution of the size and shape *versus* the arrangement of the

protein in the different regions of the scattering profile.

Guinier plots for bR in reconstituted DMPC vesicles

Guinier plots for bR in d_{63} -DMPC and d_{67} -DMPC are presented in Figure 7. These lipid-subtracted scattering profiles were acquired from the vesicles at the highest lipid-to-protein ratio ($\sim 15:1$, by weight) in buffers at the nominal contrast match points of the phospholipids. Data points are shown in the Q -range where the scattered intensity reflects the size and shape of the protein molecule and where protein-protein interference effects are insignificant. According to the well-known Guinier approximation (Guinier, 1963), the scattering profile follows the relationship $\ln[I(Q)] = - (R_g^2/3) \cdot Q^2$ in the limit as the scattering angle goes to zero so that the radius of gyration of a protein molecule can be inferred from the slope of its scattering profile at small angles. Moreover, the molecular mass of the protein molecule can be estimated from the $I(0)$ or forward scatter (Jacrot & Zaccai, 1981), which can be determined by extrapolation of the curves in Figure 7 to zero angle.

Table 1 presents a summary of the structural parameters of bR as estimated from the Guinier plots in Figure 7. Equivalent estimates of the structural parameters of bR are extracted from the scat-

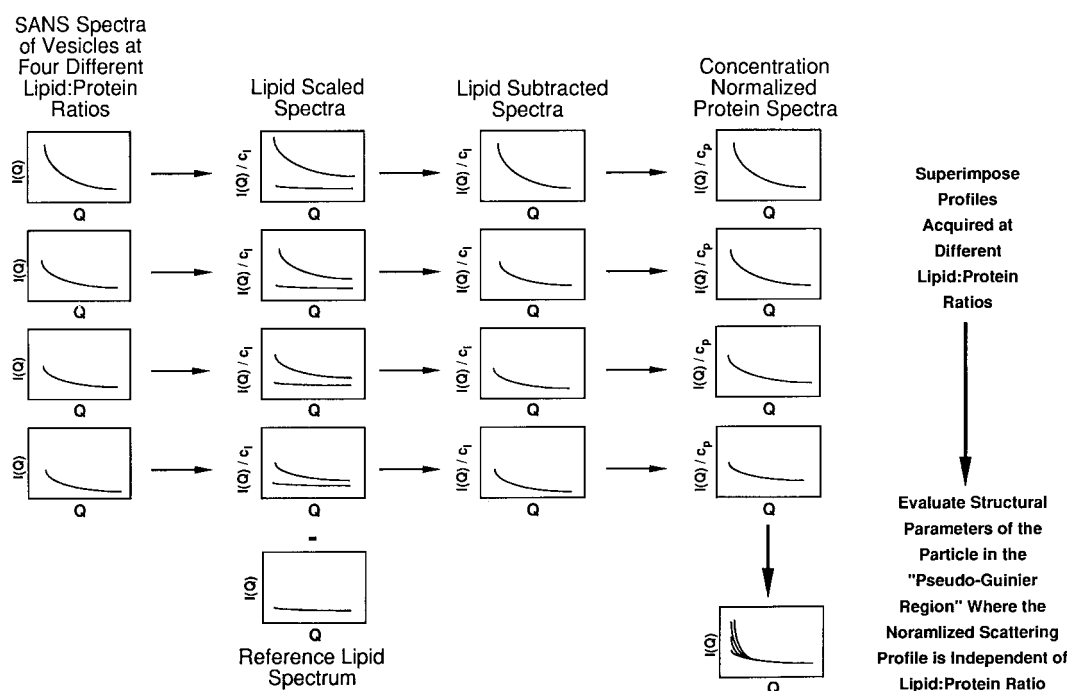


Figure 6. Summary of the processing protocol for scattering profiles acquired at the lipid contrast match point. Buffer-subtracted SANS profiles (column 1) are scaled to a specific lipid concentration (column 2 and Figure 3, above). Next, the residual scatter of the phospholipid is subtracted (column 3) and the profiles are scaled to a specific protein concentration (column 4 and Figures 4 and 5, above). The fully corrected protein profiles are compared for samples measured at different vesicle concentrations (Figure 4, above) and different protein surface densities (Figure 5, above). Finally, the scattering parameters of the protein are evaluated in a Q -range where the fully corrected protein scattering profiles are invariant (Figure 7, below).

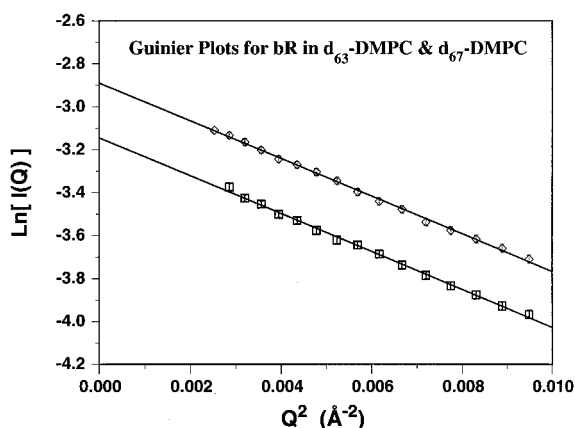


Figure 7. Guinier plots for bacteriorhodopsin in reconstituted DMPC vesicles. Protein SANS profiles were measured at a 15:1 weight ratio of lipid-to-protein either in d_{63} -DMPC vesicles at 94% $^2\text{H}_2\text{O}$ (\square) or in d_{67} -DMPC vesicles at 99% $^2\text{H}_2\text{O}$ (\diamond). This Figure shows fully corrected protein profiles, scaled to a protein concentration of 0.8 mg/ml. Error bars representing ± 1 standard deviation are shown. The sample in d_{67} -DMPC shows a higher intensity of scattered neutrons because of the higher contrast of the protein molecule in the buffer containing 99% $^2\text{H}_2\text{O}$.

tering profiles measured in the two different phospholipid environments. The data indicate a radius of gyration of either 16.3 Å (d_{63} -DMPC) or 16.2 Å (d_{67} -DMPC) and a molecular mass of either 26(± 4) kDa (d_{63} -DMPC) or 28(± 4) kDa (d_{67} -DMPC). The monomer molecular mass of bR with its covalently bound co-factor is 26.9 kDa. (Note that the offset between the two curves in Figure 7 arises from the lower contrast level of the protein in 94% $^2\text{H}_2\text{O}$ compared with 99% $^2\text{H}_2\text{O}$.)

The calculation of the molecular mass of the protein depends on assumptions as to the partial specific volume of the protein and the level of $^1\text{H}/^2\text{H}$ exchange in the protein in the $^2\text{H}_2\text{O}$ buffers used for the SANS measurements. Unfortunately, these assumptions cannot be verified independently and represent a potential limitation on the accuracy of the estimates of the molecular mass. In our calculations, we have assumed a protein partial specific volume of 0.75 cm³/g. This estimate is probably

correct within $\pm 2\%$ and almost certainly correct within $\pm 4\%$ (Zamyatin, 1984), which propagates into a maximum uncertainty of $\pm 14\%$ in the estimate of the molecular mass (Jacrot & Zaccai, 1981). We have estimated that 75% of the exchangeable protons in bR equilibrate with the $^2\text{H}_2\text{O}$ in the buffer. This estimate is based on the assumption that all of the protons in bR exchange except for approximately 15 amide protons on the backbone of each of the seven transmembrane α -helices. This assumption seems reasonable *a priori* (see Materials and Methods), and it is consistent with the level of amide exchange observed in purple membrane using polarized infrared spectroscopy (Earnest *et al.*, 1990). Nonetheless, we believe that there could be as much as a 10% error in our estimate of the exchange level, which would propagate into a $\pm 6\%$ error in the estimate of the molecular mass. Another potential source of systematic error is the quantitation of the specific activity of the radiolabel in the protein, which is only reliable to within approximately $\pm 3\%$, because of limitations on the precision of the quantitative amino acid analyses; this uncertainty propagates into an equivalent $\pm 3\%$ uncertainty in the estimate of the molecular mass. Finally, we expect a statistical uncertainty of approximately $\pm 3\%$ in our quantitation of the protein concentration in the individual SANS samples because of the limited precision of the pipetting process which is used to aliquot the samples for scintillation counting.

Given all of these uncertainties, the small discrepancies between the molecular mass of bR measured in the SANS experiments and the known monomer molecular mass of bR are insignificant. In fact, an overall level of precision of only approximately $\pm 15\%$ is expected in estimates of molecular mass based on the calibration of neutron scattering data on an absolute intensity scale (Jacrot & Zaccai, 1981). We conclude that the observed forward scatter is consistent with bR being present as a monomer in the reconstituted phospholipid vesicles.

Calculation of the theoretical R_g of bR based on the coordinates of the atomic model given by Grigorieff *et al.* (1996) predicts a value of approximately 16.7 Å for the monomer and 24.1 Å for the trimer observed in the unit cell of the two-dimen-

Table 1. Summary of the observed SANS parameters of bR in DMPC vesicles

Environment	Measured molecular mass (kDa)	Measured R_g (Å)	Theoretical R_g (Å)	
			Monomer	Trimer
d_{63} -DMPC/94% $^2\text{H}_2\text{O}$	25.6	16.3	16.7	24.1
d_{67} -DMPC/99% $^2\text{H}_2\text{O}$	28.1	16.2	16.8	24.1

The scattering parameters of bR were estimated from the Guinier plots shown in Figure 7. The calculations of the molecular mass were performed assuming 75% $^1\text{H}/^2\text{H}$ exchange and a protein specific volume of 0.75 cm³/g. The covalent molecular mass of the bR monomer is 26.9 kDa. The experimental estimate of the R_g was derived from analysis of the Guinier plot in the Q -range with $0.8 \leq Q \cdot R_g \leq 1.6$. The calculations of the theoretical R_g were performed using the protein coordinates from model 2BRD in the Brookhaven Protein Data Bank (Grigorieff *et al.*, 1996) and assuming approximately 75% $^1\text{H}/^2\text{H}$ exchange (i.e. exchange of all but approximately 15 backbone protons in the core of each transmembrane helix as described in detail in Materials and Methods); when full backbone exchange was assumed in these calculations, values of 17.1 Å and 24.3 Å were obtained for the R_g of the monomer and the trimer, respectively, independent of the solvent contrast level.

sional crystals of bR. Therefore, the experimental estimate of approximately 16.3 Å derived from the SANS measurements is consistent with expectations for the R_g of the bR monomer. However, there are several practical and conceptual complications that should be considered in interpreting this close correspondence.

It can be difficult to make an accurate prediction of the experimental R_g value of a protein even if its three-dimensional structure is known at atomic resolution (Lattman, 1989). The R_g value, especially that measured by SANS, depends on the detailed distribution of scattering length density in the molecule (Ibel & Stuhmann, 1975), which is affected by the amount and the density of bound solvent and counter-ions (Lehmann & Zaccai, 1984; Zaccai *et al.*, 1986; Zaccai, 1986), species that are not well-determined in most protein structures. Beyond these conceptual difficulties, there is a practical problem in applying the calculation to the atomic model of bR from electron crystallography because it is missing the first six residues and the final 22 residues in the mature protein molecule. These protein segments will be located at long radii relative to the center of scattering length density in the protein so that their absence means that calculations based on these coordinates will tend to underestimate the R_g value of bR. The contribution of these disordered segments to the observed R_g value will be reduced compared with what might be expected for 11% of the covalent structure because all of the exchangeable protons in these segments will equilibrate with the $^2\text{H}_2\text{O}$ in the buffer, thereby reducing their contrast level. Moreover, the retinal chromophore was omitted from the calculation of the R_g , and this omission will tend to produce a small inflation in the predicted R_g value because the chromophore resides very close to the center of scattering length density in the protein molecule. In the context of these practical ambiguities and the more fundamental ambiguities related to the behavior of bound solvent and counter-ions, we believe that there is a reasonably convincing correspondence between the measured R_g and the predicted value of the R_g of the bR monomer, although the measured value might represent a slight underestimate.

The relatively high Q -range that was used to evaluate the R_g could account for this minor discrepancy. Ideally, the radius of gyration of a particle is estimated based on analysis of the scattering data at $Q \leq 1/R_g$, i.e. $Q \cdot R_g \leq 1$ (Feigin & Svergun, 1987). Unfortunately, in our experiments, the data at very low values of Q cannot be used to estimate the scattering parameters of the protein molecule because of protein-protein interference effects in the vesicles. We have evaluated the radius of gyration of bR based on analysis of data in the range $0.8 < Q \cdot R_g < 1.6$. Our inability to use data at lower values of Q could produce a systematic error in the estimate of the R_g , and based on the observed shape of the extended scattering profile, this error would result in an underestima-

tion of the R_g . However, model calculations by Feigin & Svergun (1987) suggest that the magnitude of this error should be less than 5% in the Q -range used in our analysis.

It is important to note that essentially identical values of the R_g are obtained from measurements in both the d_{63} - and d_{67} - phospholipids. Bilayers made from the different deuterated phospholipids will have substantially different internal fluctuations in their neutron scattering length densities (Zaccai *et al.*, 1979; Büldt *et al.*, 1979, 1978; Wiener & White, 1992). We would expect to observe a difference in the scattering profile of the protein molecule in the two bilayers if protein-lipid interference effects made a significant contribution to the small angle scattering in either type of vesicle. The identical shape of the protein scattering profile in the two environments indicates that such interference effects are negligible in the relevant Q -range. We conclude that the SANS experiment is not compromised by the inability to match the neutron scattering length density of the phospholipid bilayer in detail.

Observation of chemical cross-linking *in situ*

In order to confirm that we are able to observe a change in the aggregation state of an integral membrane protein in a phospholipid bilayer, we conducted a chemical cross-linking experiment *in situ* using glutaraldehyde. After SANS profiles were measured for pure lipid vesicles and protein-containing vesicles at the contrast match point of the phospholipid, a small amount of glutaraldehyde (~1% by volume) was added to each of the samples, and their SANS profiles were measured again. Figure 8(a) shows the buffer-subtracted scattering profiles (prior to lipid subtraction). The cross-linking reagent has little effect on the residual scatter from the phospholipid but produces a dramatic increase in the intensity scattered at low angle by the protein-containing vesicles. Scattering profiles are shown for the bR vesicles at approximately one hour and five hours after the addition of glutaraldehyde; these two profiles are essentially identical, indicating that the cross-linking reaction is completed during the first hour of incubation.

Figure 8(b) shows a Guinier plot of the scattering profiles from the protein-containing vesicles after lipid subtraction and scaling according to protein concentration. A dramatic increase in the forward scatter and the average radius of gyration of the protein is observed upon the addition of cross-linking reagent. These samples were analyzed by SDS-polyacrylamide gel electrophoresis following removal from the neutron beam; approximately 50% of the protein had been converted to dimer, and a small amount had been converted to higher-order aggregates (data not shown). Therefore, the cross-linking experiment proves that the SANS profile is sensitive to the aggregation state of the reconstituted protein molecule. Furthermore, it suggests that this method could be used to charac-

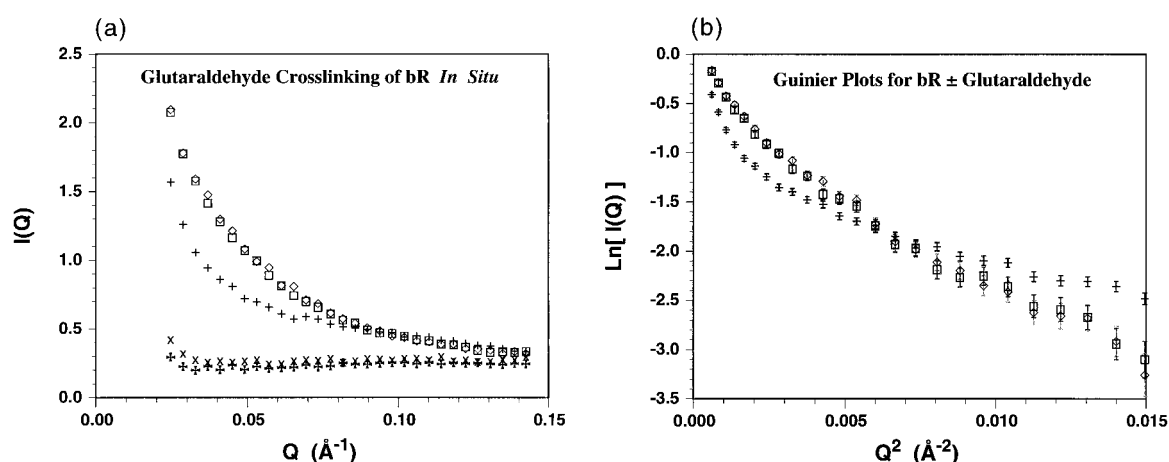


Figure 8. Chemical cross-linking of bR *in situ* in reconstituted d_{63} -DMPC vesicles. Glutaraldehyde was added to the samples and to the pure buffer to a final concentration of 1% (w/v). The samples were incubated at 35°C for one hour prior to the first SANS measurement. There was a 10:1 weight ratio of lipid-to-protein in the bR vesicles (corresponding to approximately a 400:1 molar ratio). The buffer contained 93% $^2\text{H}_2\text{O}$ prior to the addition of glutaraldehyde. (a) Buffer-subtracted profiles scaled to a phospholipid concentration of 200 mg/ml. Plots are shown for the pure lipid vesicles before (⊠) and after (×) the addition of glutaraldehyde and for the bR vesicles before (+) and after one hour (◇) and five hours (□) of glutaraldehyde treatment. (b) The protein profiles from (a) are replotted in the Guinier format following lipid subtraction (using the same symbols). The profiles are scaled to a protein concentration of 10 mg/ml. Error bars representing ± 1 standard deviation are shown.

terize functional changes in integral membrane protein aggregation state *in situ* in reconstituted phospholipid bilayers.

Discussion

The small angle neutron scattering measurements in contrast-matched DMPC bilayers indicate that bR is present as a monomer in this environment at 35°C (at a high lipid-to-protein ratio). Since previous experiments using a variety of other techniques have come to the same conclusion (Cherry *et al.*, 1978), we believe that the neutron scattering experiments presented here represent a viable approach to the determination of the aggregation state of integral membrane proteins in reconstituted phospholipid vesicles. This conclusion is reinforced by the ability to observe a chemically induced change in the aggregation state of bR *in situ* in the reconstituted DMPC vesicles.

Nonetheless, inter-particle interference effects are intrinsic to scattering experiments in reconstituted vesicles, and these effects must be examined explicitly in order to isolate a region of the neutron scattering profile which is relatively free from their influence. Reasonable estimates of the structural parameters of individual integral membrane protein molecules can be extracted from this region of the scattering profile, as long as it falls in a range of angles where the Guinier approximation is valid. In the case of the bR/DMPC vesicles at a 15:1 weight ratio of lipid-to-protein, this region occurs between $0.05 \leq Q \leq 0.01$, which corresponds to $0.8 \leq Q \cdot R_g \leq 1.6$. There should be at

most a 5% distortion in the estimate of the R_g of the protein molecule based on analysis of the scattering profile in this region (Feigin & Svergun, 1987).

An important question concerns whether this SANS method is applicable to proteins larger or smaller than bR. The range of scattering angles in which we obtained reliable data for the bR monomer would not be suitable for the analysis of a protein with a substantially larger radius of gyration. However, since the scattering power of a protein molecule is linearly proportional to its molecular mass, the scattering profile of a larger protein can be measured in vesicles at a higher lipid-to-protein ratio. In such vesicles it will be possible to obtain an undistorted protein scattering profile in a lower angular range because the magnitude of the intravesicular interference effects is inversely proportional to the lipid-to-protein ratio in the reconstituted vesicles. Under the correct conditions, it may be possible to obtain a reliable estimate of the R_g of a molecule substantially larger than bR. We believe that it should be possible to apply the SANS method in exactly the manner presented here to integral membrane protein complexes ranging in size from 10 kDa to 150 kDa.

It is worthwhile to examine in detail some of the considerations that contributed to this conclusion. We are limited in this experimental system by the angular range in which interparticle interference effects are negligible and by the intensity of neutrons scattered by the protein relative to the intensity of the residual scatter of the phospholipid. If the scattering of the protein molecule is too weak, the scaling of the protein scattering profile will be sensitive to subtraction errors due to statistical

uncertainty in counting the neutrons and quantitating the concentration of phospholipid in the samples. Based on analysis of the signal levels in our experimental data, we believe that reliable protein scattering profiles could be obtained for bR at lipid-to-protein weight ratios up to approximately 30:1 (twice as high as the highest ratio used in our experiments). Since the scattering power of a protein molecule is linearly proportional to its molecular mass (Guinier, 1963), higher lipid-to-protein ratios can be used for SANS experiments with larger proteins, and, in general, the optimal lipid-to-protein ratio will scale with the first power of the molecular mass of the protein (or the protein oligomer).

On the other hand, in the dilute limit where particle-particle distances are independent of particle size, intravesicular interference effects scale with the first power of the surface density of the protein, which is inversely proportional to the lipid-to-protein ratio in the vesicle. Since larger protein molecules can be measured at higher lipid-to-protein ratios, intravesicular interference effects will be reduced, and it will be possible to obtain an undistorted scattering profile for the protein molecule at lower values of the scattering angle. The exact angular range that will be accessible depends on both the surface density of the protein and the shape function for its distribution (see Theoretical Considerations, above). We have evaluated the shape function for the bR vesicles (data not shown); the slope of this function is very steep below $Q = 0.025$ but relatively gradual for angles in the range $0.025 \leq Q < 0.06$. Therefore, it is unlikely that it will be possible to obtain an undistorted protein scattering profile at $Q < 0.025$, even at a very high lipid-to-protein ratio, because of the steep slope of the vesicular shape function in this angular region. Given this restriction, it probably will not be possible to obtain an accurate estimate of the scattering parameters of a protein molecule with an R_g greater than 40 Å using the methods presented here.

A variety of techniques can be envisioned to correct the protein scattering profiles for the spatial arrangement of the protein molecules in the reconstituted vesicles (i.e. the intravesicular interference effect). However, since the magnitude of the interference effect is proportional to the surface density of the protein, all of the correction schemes are sensitive to errors in the estimation of this parameter. We have found that it is difficult to evaluate the surface density of the protein with sufficient accuracy. So far, we have not identified a correction protocol which yields a more reliable estimate of the scattering parameters of bR than a straightforward evaluation of the lipid-subtracted SANS profile in the region where it is independent of the lipid-to-protein ratio in the reconstituted vesicles. Application of the SANS method to very large proteins (>150 kDa) or small peptides (<10 kDa) would require the development of a reliable correction protocol.

Materials and Methods

Materials

Synthetic phospholipids were purchased from Avanti Polar Lipids (Highbluff, AL). Triton X-100 (TX-100) was purchased from Pierce (Rockford, IL) in Surfact-Amp grade; β -octylglucoside (β -og) was purchased from Sigma (St. Louis, MO); and octanoyl-*N*-methylglucamide (Mega-8) was purchased from Boehringer-Mannheim (Indianapolis, IN). All phospholipids and detergents were used without further purification. [^{14}C]DPPC was obtained from Dupont-NEN (Boston, MA). Glutaraldehyde was purchased in sealed ampoules from Sigma. Chloroform was obtained in spectrophotometric grade. The 0.22 μm pore size polycarbonate syringe filters were purchased from Costar (Cambridge, MA).

Buffers

Column chromatography and protein reconstitution were performed in 200 mM NaCl, 50 mM NaH_2PO_4 , 0.025% (w/v) NaN_3 (pH 6.0); this buffer is called Chloride HPLC Buffer (CHB). Small-angle neutron scattering experiments were conducted in $^1\text{H}_2\text{O}/^2\text{H}_2\text{O}$ buffers containing 200 mM NaCl, 38.65 mM NaH_2PO_4 , 11.6 mM Na_2HPO_4 , 0.02% (w/v) NaN (pH 6.0). The $^2\text{H}_2\text{O}$ content of all buffers is expressed in % (v/v); these solutions were made by mixing appropriate volumes of a pure $^1\text{H}_2\text{O}$ buffer and a pure $^2\text{H}_2\text{O}$ buffer. The d_{63} -DMPC vesicles were measured in a buffer containing 94% $^2\text{H}_2\text{O}$ while the d_{67} -DMPC vesicles were measured in a buffer containing 99% $^2\text{H}_2\text{O}$.

Phospholipid preparation

The synthetic phospholipid was dissolved in chloroform at 20 mg/ml, and trace [^{14}C]DPPC (less than 0.01% by mass) was added out of a stock solution in ethanol/toluene. After mixing, the solvent was removed on a Rotovap, and the lipid film was dried overnight at high vacuum (<50 mTorr) prior to being dissolved at 20 mg/ml in 3% (w/v) Mega-8 in CHB. Following sonication for one hour at approximately 45°C in a Branson 2000 bath sonicator, the stock solution was filtered through a pre-rinsed 0.22 μm pore size polycarbonate syringe filter; the yield of lipid during filtration was in excess of 99% based on scintillation counting. The stock solution was stored at -20°C pending use in reconstitutions.

Preparation of bacteriorhodopsin

Purple membrane was prepared and biosynthetically labeled with [^3H]leucine as described by Popot *et al.* (1987). The specific activity of the protein was determined using quantitative amino acid analysis. In our hands, the published procedures for the delipidation and reconstitution of bR (Huang *et al.*, 1980) that were available at the time that we initiated these studies produced protein that was at least partially denatured and aggregated by the time that it had been reconstituted into vesicles, presumably due to instability of bR in the detergents used for purification. The presence of the protein aggregates in the reconstituted vesicles rendered the small angle scattering profiles of the protein uninterpretable. These aggregates also could be detected by gel filtration chromatography in the detergent β -og following solubilization of the vesicles (see below). Therefore, a procedure was developed that produces rigorously

monodisperse protein as assayed by gel filtration chromatography. We found that bR exhibits superior stability in the detergent Mega-8, and this detergent offers the additional advantage that bR/Mega-8 mixed micelles are substantially larger than phospholipid/Mega-8 mixed micelles so that these species can be separated with baseline resolution in gel filtration chromatography on either TSK-3000SW or TSK-2000SW columns.

In a typical preparation, 15 mg of purple membrane was collected by ultracentrifugation and resuspended in 0.9 ml of buffer containing 5.0% (w/v) TX-100, 20 mM NaH₂PO₄ (pH 7.0). A small Teflon stir-bar was added to this solution, and solubilization proceeded with gentle stirring. After a minimum of 12 hours incubation at room temperature in the dark, unsolubilized membrane was removed by centrifugation at maximum speed in an A95 rotor in an Airfuge (Beckman, Palo Alto, CA) for 45 minutes at room temperature. Concentrated Mega-8 and CHB buffer salts were added to the supernatant to final concentrations of 5% (w/v) and 1X, respectively, and this solution was filtered through a pre-rinsed 0.22 μ m pore size polycarbonate syringe filter. The protein was separated from phospholipid and TX-100 by a single step of gel filtration in 2.2% (w/v) Mega-8 in CHB on a TSK-3000SW column (21 mm \times 300 mm) equipped with a TSK-SW pre-column (21 mm \times 50 mm). The protein solution (~1.8 ml) was injected, and the column was eluted at a flow-rate of 4.0 ml/min at room temperature. Protein-containing fractions were pooled and stored at 4°C pending reconstitution.

Reconstitution

Vesicles were produced by dialysis. Phospholipid and protein in Mega-8 buffer were mixed in the appropriate weight ratio (approximately 4.5:1) and transferred to SpectraPor-2 tubing for dialysis against 50 volumes of CHB at 4°C. Dialysis proceeded for a minimum of 72 hours with at least six buffer changes. Pure phospholipid vesicles were prepared in the same manner. Following reconstitution, the vesicles were collected by ultracentrifugation and resuspended in CHB at a phospholipid concentration of approximately 80 mg/ml; resuspension was accomplished by gentle vortexing in conjunction with bath sonication at 37°C over a period of approximately 30 minutes. The vesicle suspension was transferred into SpectraPor-2 tubing and dialyzed against 20 volumes of pure ²H₂O buffer for 24 hours at room temperature. Finally, the samples were dialyzed against 20 volumes of buffer with the appropriate ²H₂O content for the SANS measurement; this dialysis proceeded for 24 hours at room temperature with one change of buffer.

Vesicle manipulation during SANS measurements

In the early stages of the experiments, chronic problems were encountered due to sedimentation of the vesicles during SANS measurements, and consistent background subtraction and scaling could not be achieved. These problems were alleviated by limit sonication of the vesicles in a bath sonicator immediately prior to measurement and maintenance of the vesicles at 35°C (safely above the phase transition temperature) at all times during measurement. The samples were sonicated directly in the quartz cuvettes used for the SANS measurements which were sealed with a Teflon stopper and Parafilm. Sonication proceeded at 37° to 42°C for ten

minutes and then continued for an additional ten to 15 minutes if the turbidity in the sample seemed excessive. To confirm that appreciable sedimentation was not occurring during SANS measurements, the concentration of lipid and protein in the solution was quantitated immediately before and immediately after each measurement by scintillation counting of a small aliquot (~12 μ l) removed in a manner so as to avoid resuspending any sedimented vesicles. In all cases, the observed sample concentration before and after the measurement varied by less than 2% (i.e. within the limits of accuracy of the quantitation).

The lipid-to-protein ratio in the bR vesicles was varied by fusing them with pure lipid vesicles. Fusion was accomplished by two cycles of freeze/thaw/sonication. The vesicles were mixed directly in one of the quartz cuvettes used for the SANS measurements. The solution was frozen by immersing the bottom of the cuvette in a solid CO₂/ethanol bath, thawed in a breaker of water at room temperature, and then sonicated for five minutes (at 37° to 42°C). Following a second round of freeze/thaw in an identical manner, the vesicles were sonicated for ten minutes and then transferred to the thermally regulated sample holder.

Glutaraldehyde cross-linking

Immediately after opening a sealed ampoule, glutaraldehyde was added to the samples in the cuvettes to a final concentration of 1% (v/v). The samples were incubated for approximately one hour at 35°C prior to the first SANS measurement. The bR sample and the pure DMPC sample contained 44 mg/ml and 32 mg/ml phospholipid, respectively. A profile of glutaraldehyde-containing buffer was used for background subtraction of the profiles measured from these samples.

Quantitation of isotopic labels

A double radiolabeling scheme was employed because accurate assessment of the concentration of both the phospholipid and the protein in each sample is essential for successful data scaling. The protein contained a low-level biosynthetic label in the form of [³H]leucine, while the deuterated phospholipid preparations contained trace [¹⁴C]DPPC. ³H decay was quantitated in an energy window from 0 to 5 keV where the specific activity of the protein was approximately 40 cpm/ μ g. ¹⁴C decay was quantitated in an energy window from 10 to 100 keV where the specific activity of the phospholipid was approximately 3 cpm/ μ g. The fractional spillover in both windows was determined by counting pure protein and pure lipid samples. Scintillation counting was performed using a Tri-Carb 2000CA liquid scintillation counter (Packard, Downers Grove, IL); samples were dispersed in the scintillant Optifluor (Packard) in 7 ml glass vials. Analysis was performed on three independent aliquots of each sample (4 μ l, 8 μ l, and 12 μ l) that were collected using a Microman M-25 positive-displacement micro-pipet (Rainin, Woburn, MA).

Analytical chromatography

Analytical gel filtration chromatography was performed on a TSK-2000SW column (7.5 mm \times 300 mm) equipped with a TSK-SW pre-column (7.5 mm \times 50 mm). The column was equilibrated in CHB containing 1.5% (w/v) β -og and run at a flow rate of 0.5 ml/min at

room temperature. Following the completion of the SANS measurements, each sample was assayed for the presence of irreversibly aggregated protein using gel filtration chromatography. A 15 μ l aliquot of the sample was dissolved in 110 μ l of the β -og buffer and injected onto the column without pre-column filtration. In the samples used for the analysis of the scattering parameters of bR, at most 3% of the protein appeared in large aggregates eluting in the void volume of the column, and there was no evidence of any smaller protein aggregates.

Neutron scattering measurements

Small angle neutron scattering profiles were measured on station D11 (Ibel, 1976) at the Institut Laue-Langevin in Grenoble, France. A neutron wavelength of 10 \AA was selected using a helical slot velocity selector with 9% full-width at half-maximum. The sample-to-detector distance was either 1.54 m or 2.0 m, and the 2.5 m collimator was used. The integration time for the acquisition of SANS profiles was normalized to 500,000 monitor counts, while the integration time for the acquisition of transmission data was normalized to 30,000 monitor counts. Samples were measured in 2.00 mm path-length quartz cuvettes. The sample cells were maintained at 35°C during the SANS measurements. The profile of an aliquot of the appropriate dialysis buffer was used for background subtraction. The observed small angle scattering profiles were corrected for sample transmission, buffer scattering, and electronic background using standard subtraction protocols (Ibel, 1976; Ghosh, 1989). All of the SANS profiles presented here are plotted on an absolute-intensity scale so that the intensity of neutrons scattered at angle Q is expressed as a ratio relative to that of a 1.00 mm sample of pure H_2O (Jacrot & Zaccai, 1981; Ghosh, 1989). The scattering angle Q is defined as $4\pi\sin\theta/\lambda$ where θ is equal to 1/2 the angle of deflection and λ is the neutron wavelength. An extensive series of preliminary SANS experiments were performed on station H9B at Brookhaven National Laboratory in Upton, NY.

The use of an absolute intensity scale allows straightforward evaluation of the molecular mass of the scattering particle using the following formula (Jacrot & Zaccai, 1981):

$$M_r = \left[\frac{I(0)_{\text{sample}}}{I(0)_{\text{H}_2\text{O}}} \right] \cdot \frac{(1 - T_w)}{T_w} \cdot \frac{10^3}{4\pi \cdot C \cdot t \cdot N_A} \cdot \left[\frac{\sum b_i}{(M_r)_m} - \bar{b} \cdot \bar{v} \right]^{-2}$$

In this expression, $I(0)$ represents forward scatter, T_w is the transmission of the reference sample of H_2O , C is the concentration of the protein in mg/ml, t is the path-length of the sample cuvette in cm, N_A is Avogadro's number, $\sum b_i$ is the sum of the neutron scattering lengths of the atoms in the protein monomer, $(M_r)_m$ is the molecular mass of the protein monomer, \bar{b} is the mean neutron scattering length density of the buffer, and \bar{v} is the partial specific volume of the protein. In evaluating the molecular mass of bR in the reconstituted vesicles, we assumed that 75% of the exchangeable protons equilibrate with the solvent based on the considerations outlined in the next section.

Theoretical calculation of the R_g

The atomic model of bR from electron crystallography was used to estimate the theoretical neutron scattering

R_g using the following formula (Guinier, 1963; Feigin & Svergun, 1987):

$$R_g^2 = \frac{\sum_i \Delta b_i \cdot r_i^2}{\sum_i \Delta b_i}$$

In this expression, Δb_i represents the excess scattering length of residue i , and r_i represents the distance of the α -carbon atom of the residue from the center-of-mass of the excess scattering length in the protein. The excess scattering length represents the contrast level of the amino acid relative to the buffer and is calculated as the difference between the scattering length b_i of the amino acid (Jacrot, 1976) and the scattering length of an equivalent volume of buffer:

$$\Delta b_i = b_i - \bar{b} \cdot v_i$$

The scattering lengths of the amino acids were adjusted for individual residues in the protein molecule according to the $^1\text{H}/^2\text{H}$ exchange level assumed at each position. Standard values were used for the volumes of the amino acids, v_i (Zamyatin, 1984). The average scattering length density of the buffer, \bar{b} , was calculated using the following formula, where χ represents the volume fraction of $^2\text{H}_2\text{O}$ in the buffer (Jacrot, 1976):

$$\bar{b} = (0.0697\chi - 0.00562) \cdot 10^{-12} \text{ cm}^3/\text{\AA}^3$$

Calculations were performed using a program from Venki Ramakrishnan (University of Utah), which was modified to allow specification of the exchange level independently for each amino acid in a three-dimensional structure. The atomic coordinates for bR were taken from file 2BRD in the Brookhaven Protein Data Bank, which contains the refined structure reported by Grigorieff *et al.* (1996). Non-protein atoms were ignored in the calculation. All of the exchangeable protons were assumed to equilibrate with solvent except for approximately 15 backbone protons in the core of every transmembrane α -helix (i.e. except for the hydrogen-bonded backbone protons more than three or four residues from a helix terminus); this exchange model corresponds to an overall $^1\text{H}/^2\text{H}$ exchange level of about 75%.

Acknowledgments

The authors thank Dieter Schneider for assistance and hospitality while using station H9B at Brookhaven National Laboratory. We are also grateful to Mikio Kataoka and John Flanagan for helpful discussions and to Venki Ramakrishnan for sharing his neutron scattering software.

References

- Bendzko, P. I., Pfeil, W. A., Privalov, P. L. & Tiktopulo, E. I. (1988). Temperature-induced phase transitions in proteins and lipids. Volume and heat capacity effects. *Biophys. Chem.* **29**, 301–307.
- Bormann, B. J. & Engelman, D. M. (1992). Intramembrane helix-helix association in oligomerization and transmembrane signaling. *Annu. Rev. Biophys. Biomol. Struct.* **21**, 223–242.
- Büldt, G., Gally, H. U., Seelig, A., Seelig, J. & Zaccai, G. (1978). Neutron diffraction studies on selectively

- deuterated phospholipid bilayers. *Nature*, **271**, 182–184.
- Büldt, G., Gally, H. U., Seelig, J. & Zaccai, G. (1979). Neutron diffraction studies on phosphatidylcholine model membranes. I. Head group conformation. *J. Mol. Biol.* **134**, 673–691.
- Capel, M. S., Engelman, D. M., Freeborn, B. R., Kjeldgaard, M., Langer, J. A., Ramakrishnan, V., Schindler, D. G., Schneider, D. K., Schoenborn, B. P. & Sillers, I. Y., *et al.* (1987). A complete mapping of the proteins in the small ribosomal subunit of *Escherichia coli*. *Science*, **238**, 1403–1406.
- Carraway, K. L. & Cerione, R. A. (1991). Comparison of epidermal growth factor (EGF) receptor-receptor interactions in intact A431 cells and isolated plasma membranes. Large scale receptor micro-aggregation is not detected during EGF-stimulated early events. *J. Biol. Chem.* **266**, 8899–8906.
- Carraway, K. L., Koland, J. G. & Cerione, R. A. (1989). Visualization of epidermal growth factor (EGF) receptor aggregation in plasma membranes by fluorescence resonance energy transfer. Correlation of receptor activation with aggregation. *J. Biol. Chem.* **264**, 8699–8707.
- Casey, J. R. & Reithmeier, R. A. (1991). Analysis of the oligomeric state of Band 3, the anion transport protein of the human erythrocyte membrane, by size exclusion high performance liquid chromatography. Oligomeric stability and origin of heterogeneity. *J. Biol. Chem.* **266**, 15726–15737.
- Cherry, R. J., Moøller, U., Henderson, R. & Heyn, M. P. (1978). Temperature-dependent aggregation of bacteriorhodopsin in dipalmitoyl and dimyristoylphosphatidylcholine vesicles. *J. Mol. Biol.* **121**, 283–298.
- Cochet, C., Kashles, O., Chambaz, E. M., Borrello, I., King, C. R. & Schlessinger, J. (1988). Demonstration of epidermal growth factor-induced receptor dimerization in living cells using a chemical covalent cross-linking agent. *J. Biol. Chem.* **263**, 3290–3295.
- Curmi, P. M., Stone, D. B., Schneider, D. K., Spudich, J. A. & Mendelson, R. A. (1988). Comparison of the structure of myosin subfragment 1 bound to actin and free in solution. A neutron scattering study using actin made “invisible” by deuteration. *J. Mol. Biol.* **203**, 781–798.
- de Vos, A. M., Ultsch, M. & Kossiakoff, A. A. (1992). Human growth hormone and extracellular domain of its receptor: crystal structure of the complex. *Science*, **255**, 306–312.
- Earnest, T. N., Herzfeld, J. & Rothschild, K. J. (1990). Polarized Fourier transform infrared spectroscopy of bacteriorhodopsin. Transmembrane alpha helices are resistant to hydrogen/deuterium exchange. *Bio-phys. J.* **58**, 1539–1546.
- Feigin, L. A. & Svergun, D. I. (1987). *Structure Analysis by Small-Angle X-ray and Neutron Scattering*, Plenum Press, New York.
- Findlay, J. B., Donnelly, D., Bhogal, N., Hurrell, C. & Attwood, T. K. (1993). Structure of G-protein-linked receptors. *Biochem. Soc. Trans.* **21**, 869–873.
- Gaffney, B. J. (1985). Chemical and biochemical cross-linking of membrane components. *Biochim. Biophys. Acta*, **822**, 289–317.
- Gennis, R. B. (1989). *Biomembranes: Molecular Structure and Function*, Springer-Verlag, New York.
- Ghosh, R. E. (1989). *A Computing Guide for Small Angle Scattering Experiments*, Institut Laue-Langevin, Grenoble, France.
- Glatter, O. & Kratky, O. (1982). *Small Angle X-ray Scattering*, Academic Press, New York.
- Grigorieff, N., Ceska, T. A., Downing, K. H., Baldwin, J. M. & Henderson, R. (1996). Electron-crystallographic refinement of the structure of bacteriorhodopsin. *J. Mol. Biol.* **259**, 393–421.
- Guinier, A. (1963). *X-Ray Diffraction In Crystals, Imperfect Crystals, and Amorphous Bodies*, W. H. Freeman, San Francisco.
- Heegaard, C. W., le Maire M., Gulik-Krzywicki, T. & Moøller, J. V. (1990). Monomeric state and Ca²⁺ transport by sarcoplasmic reticulum Ca²⁺-ATPase, reconstituted with an excess of phospholipid. *J. Biol. Chem.* **265**, 12020–12028.
- Heldin, C. H. (1995). Dimerization of cell surface receptors in signal transduction. *Cell*, **80**, 213–223.
- Henderson, R., Baldwin, J. M., Ceska, T. A., Zemlin, F., Beckmann, E. & Downing, K. H. (1990). Model for the structure of bacteriorhodopsin based on high-resolution electron cryo-microscopy. *J. Mol. Biol.* **213**, 899–929.
- Huang, K. S., Bayley, H. & Khorana, H. G. (1980). Delipidation of bacteriorhodopsin and reconstitution with exogenous phospholipid. *Proc. Natl Acad. Sci. USA*, **77**, 323–327.
- Hurtley, S. M. & Helenius, A. (1989). Protein oligomerization in the endoplasmic reticulum. *Annu. Rev. Cell Biol.* **5**, 277–307.
- Ibel, K. (1976). The small angle neutron scattering station D11 at the Institut Laue-Langevin. *J. Appl. Crystallog.* **9**, 296–309.
- Ibel, K. & Stuhmann, H. B. (1975). Comparison of neutron and X-ray scattering of dilute myoglobin solutions. *J. Mol. Biol.* **93**, 255–265.
- Jacrot, B. (1976). The study of biological structures by neutron scattering from solution. *Rep. Prog. Phys.* **39**, 911–953.
- Jacrot, B. & Zaccai, G. (1981). Determination of molecular weight by neutron scattering. *Biopolymers*, **20**, 2414–2426.
- Khorana, H. G. (1988). Bacteriorhodopsin, a membrane protein that uses light to translocate protons. *J. Biol. Chem.* **263**, 7439–7442.
- Knoll, W., Ibel, K. & Sackmann, E. (1981). Small-angle neutron scattering study of lipid phase diagrams by the contrast variation method. *Biochemistry*, **20**, 6379–6383.
- Lattman, E. E. (1989). Rapid calculation of the solution scattering profile from a macromolecule of known structure. *Proteins: Struct. Funct. Genet.* **5**, 149–155.
- Lehmann, N. S. & Zaccai, G. (1984). Neutron small-angle scattering studies of ribonuclease in mixed aqueous solutions and determination of the preferentially bound water. *Biochemistry*, **23**, 1939–1942.
- le Maire M. (1986). Protein-protein interactions in membranes: concepts and the example of calcium ATPase from the sarcoplasmic reticulum. *Biochimie*, **68**, 395–400.
- le Maire, M., Aggerbeck, L. P., Monteilhet, C., Andersen, J. P. & Møller, J. V. (1986). The use of high-performance liquid chromatography for the determination of size and molecular weight of proteins: a caution and a list of membrane proteins suitable as standards. *Anal. Biochem.* **154**, 525–535.
- le Maire M., Thauvette, L., de Foresta, B., Viel, A., Beauregard, G. & Potier, M. (1990). Effects of ionizing radiations on proteins. Evidence of non-random fragmentations and a caution in the use of the

- method for determination of molecular mass. *Biochem. J.* **267**, 431–439.
- Livnah, O., Stura, E. A., Johnson, D. L., Middleton, S. A., Mulcahy, L. S., Wrighton, N. C., Dower, W. J., Jolliffe, L. K. & Wilson, I. A. (1996). Functional mimicry of a protein hormone by a peptide agonist: the EPO receptor complex at 2.8 angstroms. *Science*, **273**, 464–471.
- Malfois, M., Bonneté, F., Belloni, L. & Tardieu, A. (1996). A model of attractive interactions to account for fluid-fluid phase separation of protein solutions. *J. Chem. Phys.* **105**, 3290–3300.
- Manolios, N., Bonifacino, J. S. & Klausner, R. D. (1990). Transmembrane helical interactions and the assembly of the T cell receptor complex. *Science*, **249**, 274–277.
- Marsh, D. (1990). *Handbook of Lipid Bilayers*, CRC Press, Boca Raton, FL.
- Møller, J. V., le Maire, M. & Andersen, J. P. (1988). Use of detergents to solubilize the Ca²⁺-pump protein as monomers and defined oligomers. *Methods Enzymol.* **157**, 261–270.
- Oesterhelt, D. & Stoerkenius, W. (1971). Rhodopsin-like protein from the purple membrane of *Halobacterium halobium*. *Nature New Biol.* **233**, 149–152.
- Popot, J. L. & Engelman, D. M. (1990). Membrane protein folding and oligomerization: the two-stage model. *Biochemistry*, **29**, 4031–4037.
- Popot, J. L., Gerchman, S. E. & Engelman, D. M. (1987). Refolding of bacteriorhodopsin in lipid bilayers. A thermodynamically controlled two-stage process. *J. Mol. Biol.* **198**, 655–676.
- Racker, E., Violand, B., O'Neal, S., Alfonzo, M. & Telford, J. (1979). Reconstitution, a way of biochemical research; some new approaches to membrane-bound enzymes. *Arch. Biochem. Biophys.* **198**, 470–477.
- Tanford, C. & Reynolds, J. A. (1976). Characterization of membrane proteins in detergent solutions. *Biochim. Biophys. Acta*, **457**, 133–170.
- Tardieu, A., Veretout, F., Krop, B. & Slingsby, C. (1992). Protein interactions in the calf eye lens: interactions between β -crystallins are repulsive whereas in γ -crystallins they are attractive. *Eur. Biophys. J.* **21**, 1–12.
- Ullrich, A. & Schlessinger, J. (1990). Signal transduction by receptors with tyrosine kinase activity. *Cell*, **61**, 203–212.
- Veatch, W. & Stryer, L. (1977). The dimeric nature of the gramicidin A transmembrane channel: conductance and fluorescence energy transfer studies of hybrid channels. *J. Mol. Biol.* **113**, 89–102.
- Veretout, F., Delaye, M. & Tardieu, A. (1989). Molecular basis of eye lens transparency. Osmotic pressure and X-ray analysis of α -crystallin solutions. *J. Mol. Biol.* **205**, 713–728.
- Wells, J. A. (1994). Structural and functional basis for hormone binding and receptor oligomerization. *Curr. Opin. Cell Biol.* **6**, 163–173.
- Wiener, M. C. & White, S. H. (1992). Structure of a fluid dioleoylphosphatidylcholine bilayer determined by joint refinement of X-ray and neutron diffraction data. III. Complete structure. *Biophys. J.* **61**, 437–447.
- Zaccai, G. (1986). Measurement of density and location of solvent associated with biomolecules by small-angle neutron scattering. *Methods Enzymol.* **127**, 619–629.
- Zaccai, G., Büldt, G., Seelig, A. & Seelig, J. (1979). Neutron diffraction studies on phosphatidylcholine model membranes. II. Chain conformation and segmental disorder. *J. Mol. Biol.* **134**, 693–706.
- Zaccai, G. & Jacrot, B. (1983). Small angle neutron scattering. *Annu. Rev. Biophys. Bioeng.* **12**, 139–157.
- Zaccai, G., Wachtel, E. & Eisenberg, H. (1986). Solution structure of halophilic malate dehydrogenase from small-angle neutron and X-ray scattering and ultracentrifugation. *J. Mol. Biol.* **190**, 97–106.
- Zamyatnin, A. A. (1984). Amino acid, peptide, and protein volume in solution. *Annu. Rev. Biophys. Bioeng.* **13**, 145–165.

Edited by M. F. Moody

(Received 20 December 1996; received in revised form 1 August 1997; accepted 6 August 1997)